



Structural and low temperature transport properties of Fe₂B and FeB systems at high pressure



P. Anand Kumar^{a,*}, A.T. Satya^a, P.V. Sreenivasa Reddy^b, M. Sekar^a, V. Kanchana^b,
G. Vaitheeswaran^c, Awadhesh Mani^a, S. Kalavathi^a, N.V. Chandra Shekar^a

^a Condensed Matter Physics Division, Indira Gandhi Centre for Atomic Research, Kalpakkam, 603 102, Tamil Nadu, India

^b Department of Physics, Indian Institute of Technology Hyderabad, Kandi, 502 285, Sangareddy, Telangana, India

^c Advanced Center of Research in High Energy Materials, University of Hyderabad, Gachibowli, 500 046, Telangana, India

ARTICLE INFO

Keywords:

High pressure
Low temperature
X-ray diffraction
Resistivity
Phase transition

ABSTRACT

The evolution of crystal structure and the ground state properties of Fe₂B and FeB have been studied by performing high pressure X-ray diffraction up to a pressure of ~24 GPa and temperature dependent (4.2–300 K range) high-pressure resistivity measurements up to ~2 GPa. While a pressure induced reversible structural phase transition from tetragonal to orthorhombic structure is observed at ~6.3 GPa in Fe₂B, FeB has been found to be stable in its orthorhombic phase up to the pressure of 24 GPa. In the case of Fe₂B, both parent and daughter phases coexist beyond the transition pressure. The bulk modulus of FeB and Fe₂B (tetragonal) have been found to be 248 GPa and 235 GPa respectively. First principle electronic structure calculations have been performed using the present experimental inputs and the calculated ground state properties agree quite well with the major findings of the experiments. Debye temperature extracted from the analysis of low temperature resistivity data is observed to decrease with pressure indicating softening of phonons in both the systems.

1. Introduction

Transition metal borides form intermetallic compounds which are hard, chemically inert and stable over a wide temperature range [1–4]. It has been long predicted that short covalent bonds formed by the boron atoms in metal lattice and high valence electrons of transition metal atoms make these materials highly incompressible and hard [5]. The structure of these intermetallics depends on the boron content and its arrangement in the transition metal lattice. A plethora of boron arrangements viz., isolated atoms, chains, nets and three dimensional networks are possible depending on the boron content which give rise to variety of structural ground states in these borides [5,6]. Most of these compounds are structurally stable under pressure [7]. However, the experimental reports are sparse and scattered.

Among the boride systems, iron borides have attracted a lot of attention owing to their technological applicability as hardening agents in steels [8], hard protective coatings due to their high chemical and wear resistance [1] and also as important shielding materials in nuclear reactors [9]. Since the discovery of superconductivity in MgB₂ [10] with a T_c of 39 K, studies on the transport behaviour in borides has been revived by scientific community which culminated in the discovery of

several of the superconducting boride systems [11]. Kolmogorov et al. [12], have predicted several new binary iron boride systems in addition to the known and stable Fe₂B and FeB systems with a variety of structural and magnetic ground states. Subsequently, Gou et al. [13], successfully synthesized one of their predicted compounds FeB₄ at high pressure and found phonon mediated superconductivity with T_c ~ 2.9 K and superhardness with nano indentation hardness of ~62 GPa. The increased interest after the discovery of superhardness and superconductivity in this material led many researchers to further investigate structural, mechanical and electronic properties of known stable binary borides by first principle calculations [14–16]. However there are very few experimental studies on the structural [17,18], transport and electronic properties [19–21] of these stable binary borides under. Among iron borides only Fe₂B has been studied for its structural stability under pressure. Fe₂B is found to be unstable under mechanical grinding followed by annealing [17]. However, high pressure structural study of Fe₂B does not show any such phase transitions [18]. The calculated bulk modulus on Fe₂B from first principle is found to be 249.7 GPa [22]. Whereas a similar high pressure structural study on FeB is nonexistent. The calculated bulk modulus on FeB from first principle is found to be 250 GPa [23]. In this article, we present the results of our high pressure X-ray diffraction at

* Corresponding author.

E-mail address: ak_police@igcar.gov.in (P.A. Kumar).

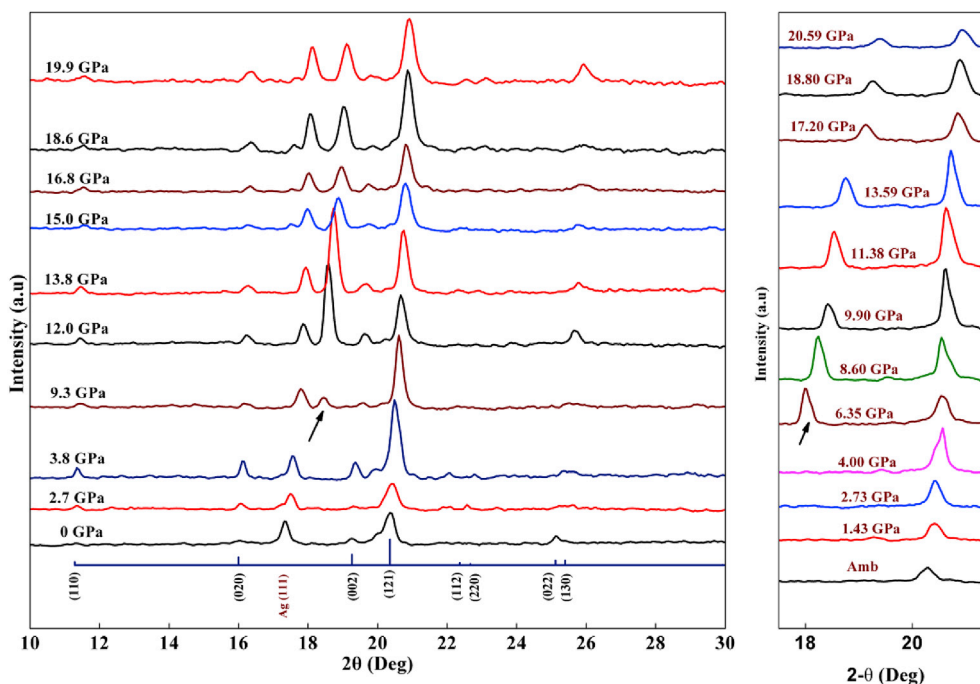


Fig. 1. High pressure XRD pattern for Fe_2B . The arrow indicates the appearance of a new peak. (a) with Ag as pressure calibrant. (b) with ruby as pressure calibrant.

ambient temperature, high pressure electrical resistivity as a function of temperature and first principle calculations on Fe_2B and FeB systems to understand the structural stability and transport behaviour.

2. Experimental and computational methods

Fe_2B (99% pure) and FeB (99% pure) powders procured from M/s Alfa Aesar were initially characterized by powder diffractometer using image plate based mar345dtb detector. The sample to detector distance was calibrated with standard LaB_6 . The single phase Fe_2B with tetragonal structure ($I4/mcm$) showed the lattice parameters $a = 5.185 \text{ \AA}$ and $c = 4.136 \text{ \AA}$ at ambient pressure which agreed well with ICDD standard pattern (PDF card no.00-036-1332). The single phase FeB with orthorhombic structure ($Pbmm$) showed the lattice parameters $a = 4.062 \text{ \AA}$, $b = 5.505 \text{ \AA}$ and $c = 2.947 \text{ \AA}$ that agrees well with ICDD standard pattern (PDF card no.04-003-3263). High pressure X-ray diffraction (HPXRD) studies were performed in a Mao-Bell type diamond anvil cell (DAC) in angle dispersive X-ray mode with a rotating anode X-ray generator (Rigaku-ULTRAX-18) with Mo target ($\lambda = 0.7107 \text{ \AA}$) up to a pressure of ~ 20 GPa. A micro focus based HPXRD system was used for studying the X-ray diffraction of FeB up to 24 GPa [24]. In both the cases an image plate based mar345dtb detector was used for data collection. The two dimensional X-ray diffraction patterns were integrated using the program FIT2D [25]. Sample loading in the pressure cell was carried out as per the following protocol. Stainless steel (SS) gaskets were pre-indented to a thickness of $\sim 60 \text{ \mu m}$ and a hole of diameter 300 \mu m was drilled at the centre of the compressed area for mounting the sample. A mixture of methanol, ethanol and water (MEW) in the volume ratio 16:3:1 was used as pressure transmitting medium. High-pressure resistivity measurements as a function of temperature in the 4.2–300 K temperature range on polycrystals of Fe_2B and FeB were carried out in a home-built, opposed anvil pressure-locked cell up to a pressure of 2 GPa. Steatite was used as the pressure transmitting medium and pyrophyllite washers were used as gasket. The internal pressure of the cell was pre-calibrated by measuring the shift in the superconducting transition temperature of lead with respect to the applied load prior to mounting the samples. An error of ~ 0.2 GPa in the reported pressure can be expected. For HPXRD experiments the sample to detector distance is calibrated to be 138.5 mm.

The collection time for each experiment was around 3 h. Further details about the sample assembly and measurements on different samples can be found in Ref [26–28].

Details of the electronic structure calculations carried on Fe_2B and FeB are as follows. The planewave pseudopotential formalism of DFT implemented within the QUANTUM ESPRESSO [29] code was used for structural and volume optimization of the present compounds. The Generalized Gradient Approximation (GGA) to the exchange correlation functional was chosen for all calculations and the electron-ion interaction was described using norm-conserving pseudopotentials. The maximum planewave cut-off energy was set at 140 Ry and the electronic charge density was expanded up to 560 Ry. A $16 \times 16 \times 16$ k-point grid within the Brillouin zone (BZ) was used for the calculations. Gaussian broadening of 0.01 Ry was used in the present calculations. The Full Potential Linearized Augmented Plane Wave (FP-LAPW) method as implemented in Wien2k code [30] was used to calculate the band structure properties of the Fe_2B and FeB with Generalized Gradient Approximation (GGA) of Perdew-Burke-Ernzerhof (PBE) [31]. The wave functions were expanded up to angular momentum $l = 10$ inside the muffin-tin spheres. The radii of muffin tin spheres, (R_{MT}) were 2.26, 1.72 a.u for Fe and B atoms respectively and the plane wave cut off energy used was $K_{\text{max}} = 7/R_{\text{MT}}$, where R_{MT} is the smallest radius of muffin tin and K_{max} is the corresponding of the largest magnitude in the plane wave expansion. All the electronic structure calculations were performed with $44 \times 44 \times 44$ k-mesh in the Monkhorst-Pack [32] scheme which gave 5963 k-points in body centered tetragonal (bct) Fe_2B case, 12167 k-points in orthorhombic Fe_2B and FeB in the irreducible part of the Brillouin Zone (BZ). Tetrahedron method [33] was used to integrate the Brillouin zone. Energy convergence of 10^{-5} Ry was used to ensure proper convergence of the self-consistent calculation in both the compounds.

3. Results and discussion

3.1. High pressure structural studies

The HPXRD patterns of Fe_2B at different pressures from 0 to 20 GPa are shown in Fig. 1. The Bragg peaks of the parent body centered tetragonal (bct) phase at ambient pressure are indicated by the stick plot.

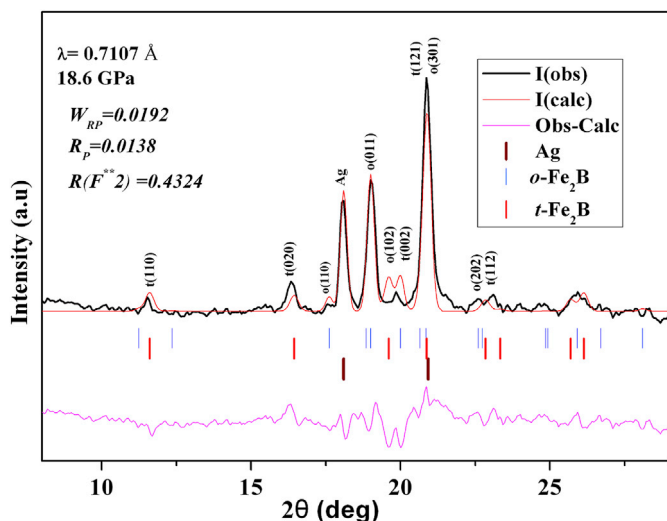


Fig. 2. Rietveld fit for the HPXRD pattern at a pressure ~ 18.6 GPa for Fe_2B system. The tick marks represent the different phases. Also indicated are the prominent peaks, tetragonal and o-orthorhombic.

The (111) of Ag peak used as pressure calibrant is also indicated in the plot. The ambient pressure tetragonal structure ($I4/mcm$) was found to be stable up to a pressure of ~ 9 GPa and above this pressure a new peak started appearing at $2\theta \sim 18.4^\circ$ and just after Ag (111) peak indicating a structural phase transition. Notice in this run there is a huge jump in pressure from 3.8 GPa to 9.3 GPa.

Subsequently, the HPXRD experiments were repeated with ruby as pressure calibrant shown in Fig. 1(b). Once again a new peak at $2\theta \sim 18.0^\circ$ was observed at around 6.3 GPa. To further rule out that the observed peak is from ruby, the HPXRD experiments were conducted without any pressure calibrant and the new peak was also observed in these measurements which confirm the authenticity of a structural phase transition. From these set of experiments it could be established that pressure at which phase transition occurs is around 6.3 GPa. The parent phase continues to be present along with the new phase up to the highest pressure studied i.e., 20 GPa. The new peak in all these experiments starts as a dot at around 6.3 GPa as observed on the image plate indicating a kind of nucleation. This dot becomes ring as pressure is increased. In all these experiments it is also observed that the peak appearing at $2\theta \sim 18^\circ$ disappears in decompression cycle. The phase transition is reversible as the parent phase alone is recovered in the ambient XRD pattern when the sample is decompressed back to the ambient pressure. Earlier study by Chen et al. [18], did not report any phase transition up to the pressure of 50 GPa. The high pressure XRD patterns by Chen et al., have reported absence of peaks because of preferred orientation. It is to be pointed out that strong peaks like (002), (020), (022) and (130) are absent in their XRD patterns. Also the 2-theta value of the new peak observed in the present work is very close to the Au 2-Theta. Also to be noticed is the increase in intensity of Au peak at high pressure in the work of Chen et al. This suggests that the new high pressure orthorhombic phase might have been coexisting even in their work. There is an interesting study by Torres et al. [17], which points out a possibility of an orthorhombic phase

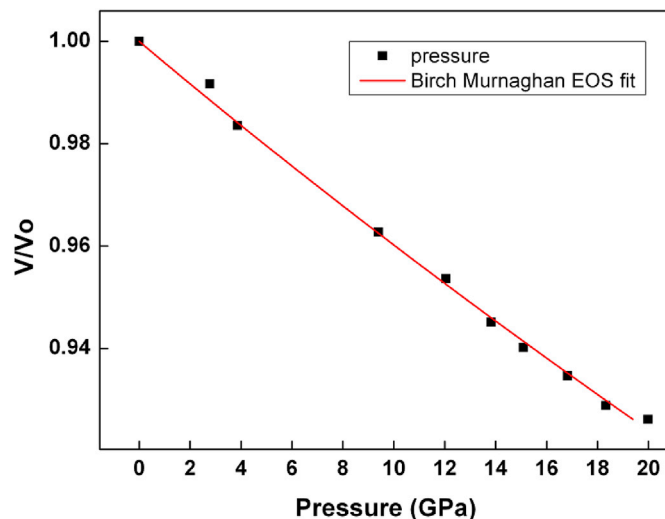


Fig. 3. Volume vs Pressure of the parent tetragonal phase of Fe_2B . The square dots are experimental data and the line is the third order fit to the Birch-Murnaghan equation of state.

of Fe_2B during mechanical grinding. It is expected that a similar metastable state to be present under static high pressure. It is known that the stable transition metal semi borides already reported in the literature, namely Fe_2B , Co_2B , Ni_2B , W_2B , Ta_2B , Mn_2B and Mo_2B crystallize in $I4/mcm$ space group; Cr_2B crystallizes in $Fddd$ space group and Mn_2B crystallizes in both $I4/mcm$ and $Fddd$ space group. The search for the space group of the daughter phase was done among the above borides. While the ambient pressure Fe_2B correspond to bct, $I4/mcm$. The high pressure orthorhombic phase did not confirm to $Fddd$ space group. Then the search was extended to include binary carbides and nitrides of transition metals of A_2B type. High pressure XRD pattern corresponding to 18.6 GPa is shown in Fig. 2. It could be best indexed with a mixture of tetragonal parent structure, space group $I4/mcm$ with lattice parameters $a = 4.986$ Å and $c = 4.135$ Å and an orthorhombic phase of Fe_2C type, space group $Pnmm$, with lattice parameters $a = 6.603$ Å, $b = 2.479$ Å and $c = 4.339$ Å. The lattice parameters were arrived at by considering the 2θ position of the new peaks respectively at 17.61° and 19.00° and in combination of three other 2θ positions respectively at 19.85° , 20.86° and 25.92° of parent phase which gave a best FOM(5) of 60. Rietveld refinement was carried out for the above high pressure X-ray diffraction data using the GSAS + EXPGUI software package [34,35] and with above obtained lattice parameters of orthorhombic structure. The refinement was performed by considering the parent phases of tetragonal Fe_2B , Ag and the orthorhombic Fe_2B phase of Fe_2C type. Considering the fact that the data is obtained at 18.6 GPa and consisting of coexisting phases of Fe_2B , the fitting is reasonably good. Table 1 lists the refined parameters along with the figure of merits.

The R parameters are $W_{RP} = 0.0192$; $R_p = 0.0138$; $R(F^{**2}) = 0.4324$.

Fig. 3 shows the pressure-volume relation of the parent phase with respect to pressure fitted to the third order Birch-Murnaghan equation of state.

Table 1
Result of the Rietveld refinement for the data collected at 18 GPa for Fe_2B .

Phase	atoms	atom coordinates	Space Group	Refined lattice parameters	Phase Fraction
Fe_2B	Fe1	(0.66,0.25,0)	$Pnmm$	$a = 6.500(6), b = 2.473(7), c = 4.360(4)$	56
	B2	(0,0,0)			
Fe_2B	Fe	(0.1581,0.681,0)	$I4/mcm$	$a = 4.969(2), c = 4.174(4)$	33
	B	(0,0,0.25)			
Ag	Ag	(0,0,0)	$Fm-3m$	$a = 3.913(1)$	11
Common factors	$U_{iso} = 0.025$	$W_{RP} = 0.0192$	$R_p = 0.0138$	$R(F^{**2}) = 0.4324$	

Table 2
Calculated lattice parameters, bulk modulus and magnetic moment of Fe atom in bct-Fe₂B and FeB compared with experimentally obtained values (*-present work).

Parameters	Experimental	Calculations
Fe₂B		
a (Å)	5.185*, 5.107 [38]	5.077*, 5.056 [14], 5.110 [39]
c (Å)	4.316*, 4.251 [38]	4.254*, 4.232 [14], 4.249 [39]
B (GPa)	235*, 164 [18]	250.3*, 249.73 [22], 244.59 [40]
Magnetic moment of Fe (μ _B)	1.62 [38]	2.0*, 1.90 [14], 1.95 [39]
FeB		
a(Å)	4.062*	3.894*
b(Å)	5.505*	5.188*
c(Å)	2.947*	3.101*
Magnetic moment of Fe (μ _B)		1.13*, 1.26 [39]

Table 3
Calculated and experimental atomic positions of bct-Fe₂B. (*-present work).

Atomic positions	Experimental	Theory
Fe (8h)	(0.1581, 0.6581, 0.0)	(0.1673, 0.6673, 0.0)*
B (4a)	(0.0, 0.0, 0.25)	(0.0, 0.0, 0.25)*

$$P(x) = \frac{3B_0}{2} [x^{\frac{7}{3}} - x^{\frac{5}{3}}] \left\{ 1 + \frac{3}{4}(B'_0 - 4) \right\} [x^{\frac{5}{3}} - 1]$$

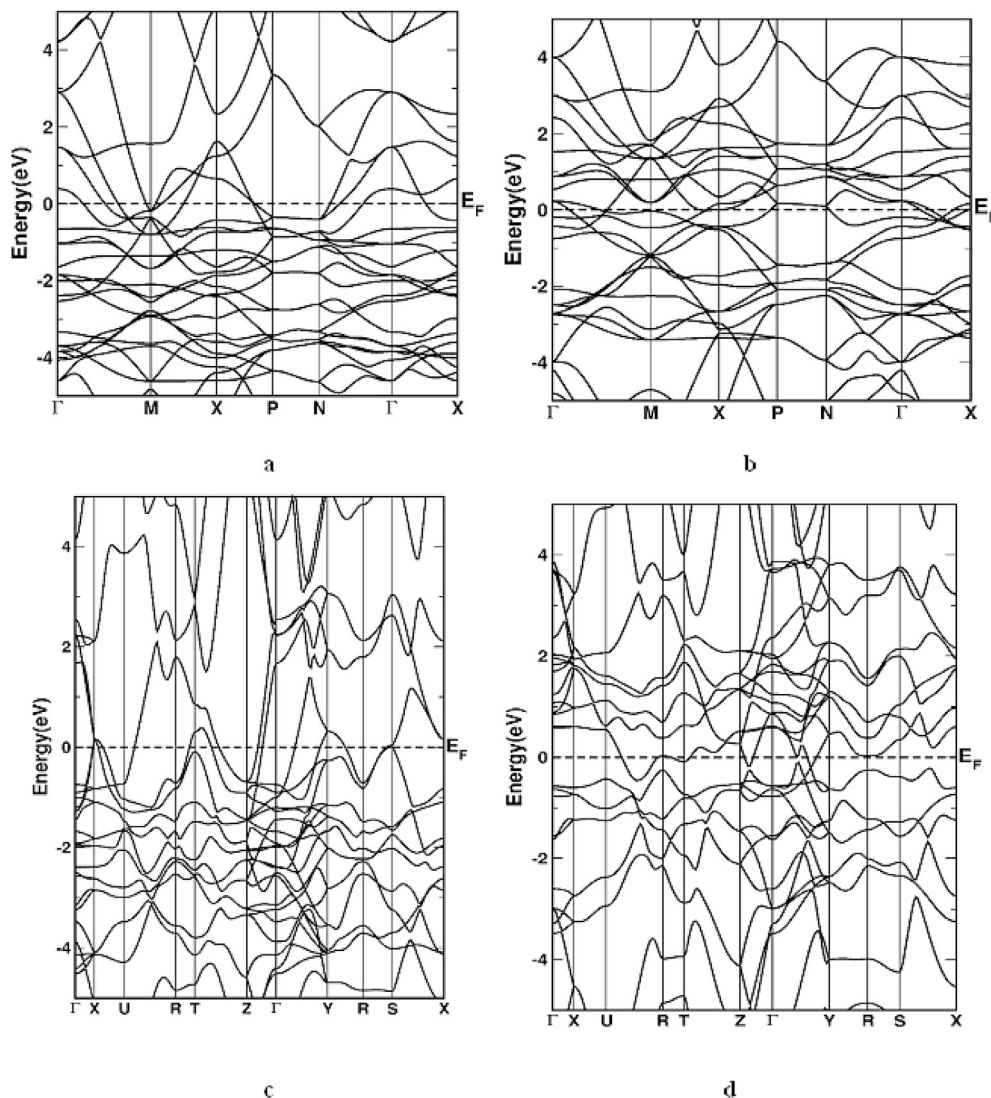


Fig. 4. Band structure of tetragonal-Fe₂B (a) Majority spin case (b) Minority spin case. Band structure of orthorhombic-Fe₂B (c) Majority spin case (d) Minority spin case.

FeB HPXRD

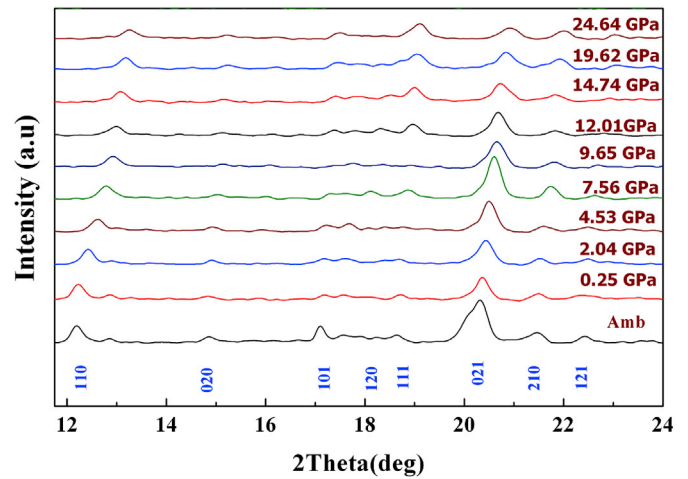


Fig. 5. High pressure XRD pattern of FeB up to a pressure of 24 GPa.

where $x = \frac{V}{V_0}$
Bulk modulus B_0 and its derivative B'_0 were found to be 235(2) GPa

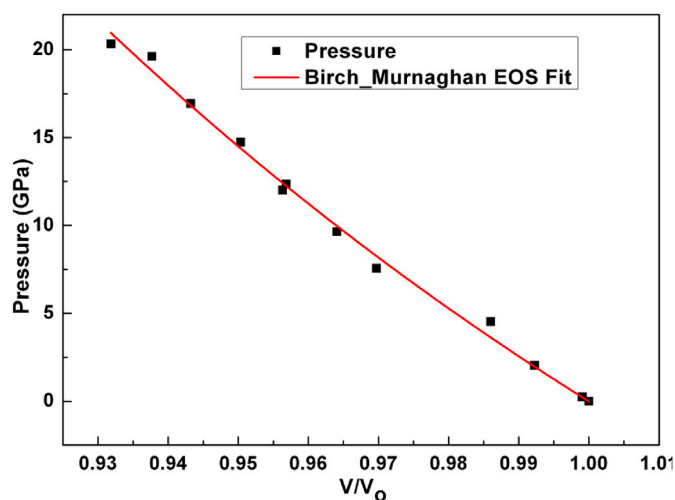


Fig. 6. Pressure vs Volume EOS fitting of FeB. The square dots indicate the experimental data. The line is the 3rd order fit to the Birch-Murnaghan equation of state.

Table 4

Result of the Rietveld refinement for FeB at 24.64 GPa.

Phase	atoms	atom coordinates	Space Group	Refined lattice parameters
FeB	FE1	(0.1157,0.175,0.25)	<i>Pbnm</i>	a = 3.981(7), b = 5.340(7), c = 2.894(8)
	B2	(0.688,0.0328,0.25)		
Common factors	$U_{iso} = 0.025$	$W_{Rp} = 0.0142$	$R_p = 0.0112$	$R(F^{*2}) = 0.1336$

and 2 respectively.

The bulk modulus of the tetragonal parent phase compares well with the computational value of 249.73 GPa [22]. The value obtained is also similar to what was reported for the other semi borides, 236.8 GPa and 302 GPa respectively for Ni_2B [36] and Mo_2B [37]. It is pertinent to note that the bulk modulus reported by Chen et al. [18], is 164 GPa which is very less compared to the calculated value.

Total energy calculations were performed for Fe_2B in body centered tetragonal structure at ambient condition. The experimental structure details were taken as inputs and the optimized lattice parameters and

atomic positions are given in Tables 2 and 3. The experimental and computational values obtained in various other works are also given in these tables for comparison.

From our calculations Fe_2B is found to possess a magnetic moment of around $2.0 \mu_B$ for Fe atom which is in agreement with other similar computational studies. The calculated bulk modulus obtained by fitting the EOS is 250.3 GPa. This is in good agreement with the observed experimental value of 235 GPa and with the reported value of 249.73 GPa [22]. The calculated Fe-Fe distances are 2.411, 2.436, 2.674 and 2.724 Å. The calculated Fe-B distance is 2.169 Å and B-B distance is 2.127 Å and they are in agreement with the values obtained by Ching et al., [39]. Calculated band structure for both majority and minority spin is given in Fig. 4(a) and (b). From this, it is observed that four bands cross the Fermi level (E_F) in the case of majority spin and three bands cross the same Fermi level in the case of minority spin. In both the spin cases, band structure is of complex nature at the high symmetry point M. It is found that bands are degenerate along P-N direction for both the spin cases and the degeneracy is lifted along other directions.

Experimentally a structural phase transition is observed from bct to orthorhombic structure at a pressure of around 6.3 GPa with space group

Pnmm (No. 58). Band structure calculations have been carried out for the orthorhombic phase too and this phase is also found to be magnetic in nature. The value of the magnetic moment on the Fe site is $2.4 \mu_B$ which is larger as compared to the corresponding bct structure. The calculated Fe-Fe distances are 2.449 and 2.767 Å. For Fe-B, the distances are 2.329 and 2.491 Å. The calculated B-B distance is 2.474 Å. No other reports are available to compare the magnetic moment in orthorhombic structure at the mentioned pressure. The calculated band structure for both majority and minority spin cases for Fe_2B in the orthorhombic structure are presented in Fig. 4(c and d). From the band structure, metallic nature of this

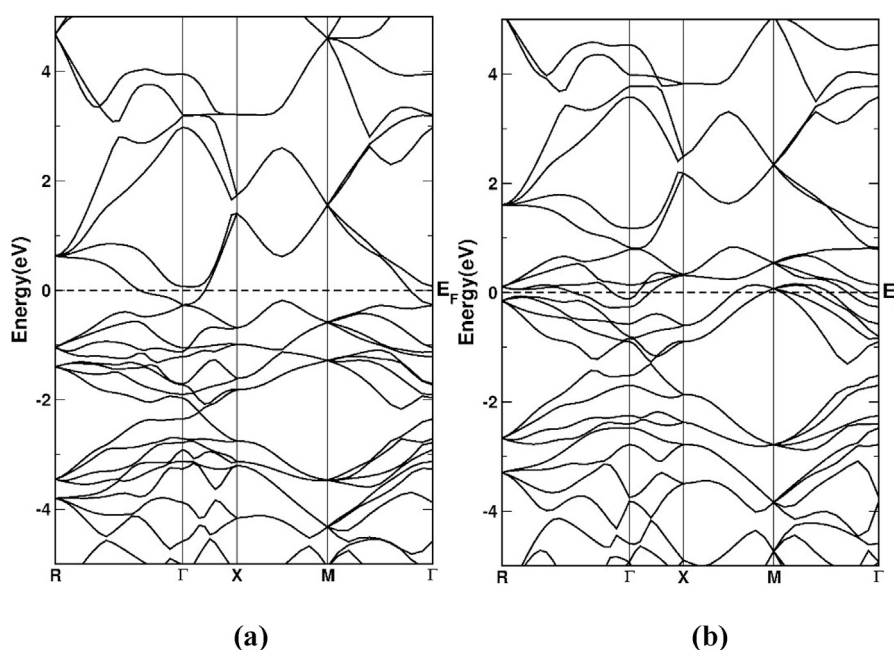


Fig. 7. Band structure for FeB in orthorhombic structure (a) majority spin and (b) minority spin.

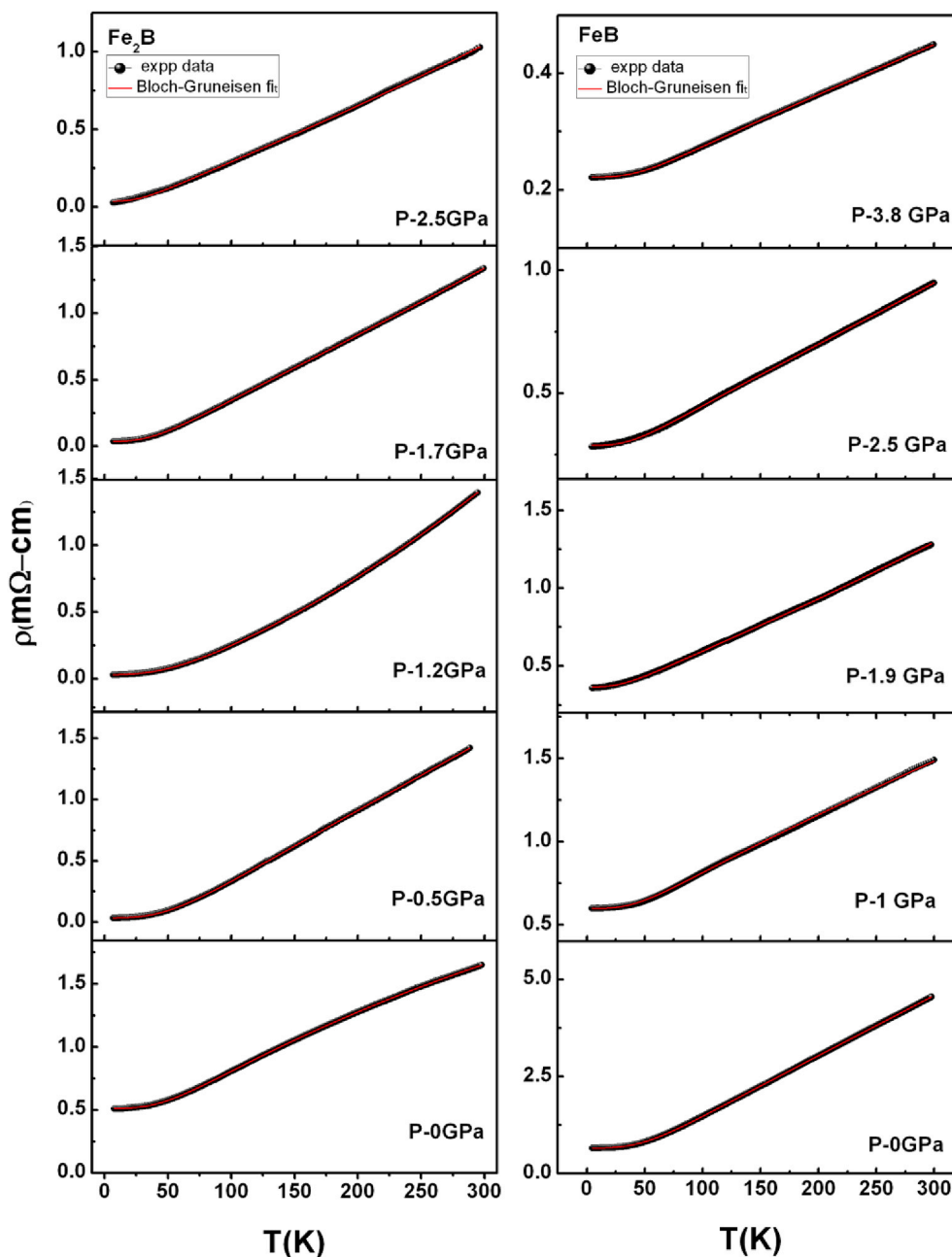


Fig. 8. Resistivity versus temperature for Fe₂B (left panel) and FeB (right panel) at different pressures. Solid spheres are experimental data points and red solid curves are fits to Bloch-Grüneisen equation. (For interpretation of the references to colour in this figure legend, the reader is referred to the web version of this article.)

phase is quite evident as the bands are found to cross the E_F . It is observed that six bands cross the E_F in the majority spin case but in the minority

Table 5

Result of the analysis of resistivity data. (as described in the text).

P(GPa)	ρ_0 (Ω -cm)	ρ_{em} (Ω -cm/ K^2)	ρ_{ph} (Ω -cm)	Θ_D (K)
Fe ₂ B				
0	1.12E-4	3.08E-9	0.00344	343(2)
0.5	3.48E-5	1.15E-9	0.00366	381(2)
1.2	3.01E-5	1.48E-9	0.00303	394(3)
1.7	3.72E-5	1.72E-9	0.00227	337(4)
2.5	3.71E-5	2.27E-9	0.00115	330(3)
FeB				
0	6.57E-4	2.94E-9	0.00980	377(3)
1	5.98E-4	2.71E-9	0.00203	318(3)
1.9	3.75E-4	2.01E-9	0.00116	315(3)
2.5	2.87E-4	1.92E-9	0.00121	313(4)
3.8	2.21E-4	1.27E-9	0.00051	334(3)

spin case it is reduced to two bands. In minority spin case double degeneracy is observed in all the directions except along Z- Γ -Y direction, for the bands which cross E_F .

We now report here the experimental and computational study on FeB. For this set of high pressure XRD experiments shown in Fig. 5, we have used ruby as a pressure calibrant and an error of 1 GPa in the measurement is expected.

We have not found any structural transition and the orthorhombic phase (space group $Pbnm$) is found to be stable up to 24 GPa. With increasing pressure the lattice parameters decrease monotonically.

The pressure-volume relation is shown in Fig. 6. The third order Birch-Murnaghan equation of state fitting of pressure vs volume yields the bulk modulus B_0 of 248(3) GPa and its derivative B'_0 of 5. The obtained bulk modulus is close to the theoretically calculated bulk Modulus of 250 GPa [23]. Table 4 provides the reitveld refinement values for the highest pressure of FeB.

Calculations are performed for FeB which crystallizes in orthorhombic structure with space group $Pbmm$ (no: 62) with atomic positions Fe (0.18, 0.25, 0.625) and B (0.036, 0.25, 0.11). We have optimized the structural parameters starting with the above mentioned experimental parameters and the values are given in Table 2 along with the experimental parameters from the current work and the values are given in Table 2. The calculated magnetic moment for Fe atom is $1.13 \mu_B$ which is in good agreement with that available in the literature [39] namely $1.26 \mu_B$. Similarly, the calculated bulk modulus of ~ 255 GPa for orthorhombic FeB agrees with our experimental bulk modulus of 248 GPa. FeB forms a layered structure made up of Fe and B layers. The calculated Fe-Fe distances in a layer are 0.775, 2.489 and 3.034 Å and Fe-Fe distance between the layers is 2.651 Å. In the same way B-B distances in the layer are 0.868, 2.063 and 2.489 Å. The calculated Fe-B distance in a layer are 0.919, 1.605, 1.693 Å.

Band structures for both majority and minority spin cases are given in Fig. 7 where it is observed that FeB shows metallic nature in both the cases due to crossing of a single band in the case of majority spin and six bands in the case of minority spin at E_F . In both the cases we have observed that the bands at R point possess multiple degeneracy which is lifted at other high symmetry directions.

3.2. High pressure-low temperature resistivity studies

The resistivity versus temperature in the range 4.2–300 K for Fe_2B sample at different pressures from 0 to 2.5 GPa is shown in the left panel of Fig. 8. At ambient pressure the system shows positive temperature coefficient of resistance typical of a metal. As the pressure increases the resistivity decreases at all temperatures systematically. The functional dependence of resistivity with temperature $\rho(T)$, is analyzed at different pressures using the following expression applicable to a conventional metal in accordance with the Matthiessen's rule [41–44].

$$\rho(T) = \rho_0 + \rho_{em}T^2 + \rho_{ph}(T)$$

$$\text{where } \rho_{ph}(T) = C \left(\frac{T}{\Theta_D} \right)^n \int_0^{\frac{\Theta_D}{T}} \left[\frac{x^n dx}{(e^x - 1)} (1 - e^{-x}) \right]$$

In the above equation, ρ_0 is the contribution to the resistivity due to electron scattering from impurity and defects which is temperature independent, ρ_{em} is the resistivity contribution from electron-electron

scattering and also from spin fluctuations [42,44], ρ_{ph} is the Bloch-Grüneisen function which represents resistivity contribution from the electron-phonon scattering. Θ_D is the Debye temperature in the above expression and C is a constant. The coefficient n takes the value 5 for elemental nonmagnetic systems and for transition metal systems, n value can be 2, 3 or 5 [43,45]. Bloch-Grüneisen function has been used to analyze the resistivity behaviour due to electron-phonon interaction in many borides [46,47] and also in other systems [43,48] and the value of Debye temperature estimated is also in agreement with the value as obtained from specific heat measurements in these systems. We have fitted the experimental data to the above equation with n value as 3 and setting the constraint that the constants ρ_0 , ρ_{em} and C are all positive. The fits are shown as red solid curves in Fig. 8(a) and constants extracted from the fits are given in Table 5. The errors obtained for ρ_0 , ρ_{em} and C from the fits were not indicated in Table 5, as they are smaller by two orders in magnitude.

From the fitting, the value of ρ_{em} was found to be of the order of 10^{-9} which indicates that electron-electron and electron-magnon interactions are not very significant in this system and the dominant contribution to resistivity arises because of electron-phonon scattering. The Debye temperature Θ_D has been extracted from the fit and is found to be ~ 343 K at ambient pressure. This value is smaller as compared to the value derived from computations [14,15,49]; however it is comparable to value extracted from specific heat measurements [50]. The variation of the Debye temperature Θ_D as a function of pressure is shown in Fig. 9(a).

Θ_D initially increases to 390 K as pressure increases to 1.2 GPa and then it decreases to 210 K as the pressure is increased to 2.5 GPa. At present the reason for this behaviour is not known and such kind of non-monotonic behaviour of Θ_D as a function of pressure was observed in alkali-halide systems [51].

The variation of resistivity for FeB system as a function of temperature at different pressures from 0 to 3 GPa is shown in the right panel of Fig. 8. This system also exhibits metallic behaviour as function of temperature; however, the value of resistivity is larger as compared to that in Fe_2B system. As in the case of Fe_2B , in this system also resistivity decreases with increase of pressure at all temperatures. We have carried out similar analysis for $\rho(T)$ behaviour in this system as we did for Fe_2B and observe again the electron-electron and electron-magnon interactions are found to be very small. The value of Debye temperature Θ_D was found to be 370 K and it is comparable to the value reported from specific heat

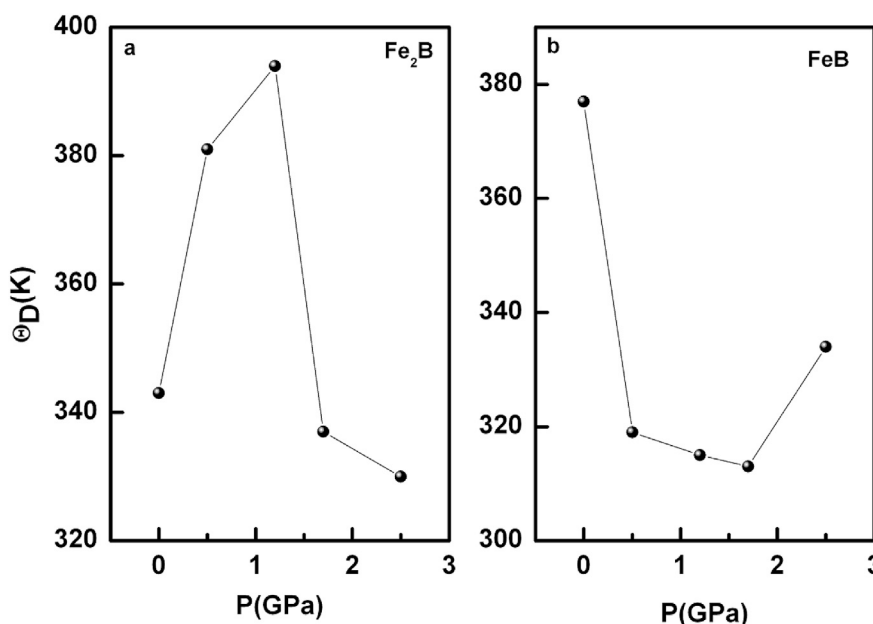


Fig. 9. Debye temperature versus pressure for Fe_2B and FeB sample at different pressures. (a) Variation of Debye temperature of Fe_2B with pressure. (b) Variation of Debye temperature of FeB with pressure.

measurements [50]. The variation of Θ_D as a function of pressure is shown in Fig. 9(b). Θ_D shows non monotonic variation with increase of pressure. It decreases to 313 K as the pressure increases to 2.5 GPa and again increases to ~ 334 K at $P \sim 3.8$ GPa.

The decrease of Debye temperature with increase in pressure in these two systems Fe_2B and FeB is surprising as normally phonons get hardened with application of pressure. The reason for phonon softening behaviour is presently not known. Kumari et al. [52] have predicted that depending on the difference of pressure derivative of isothermal and adiabatic bulk moduli, the increase or decrease of Debye temperature is possible in a given system. It can also be interpreted as arising from anisotropy in electron phonon coupling in different symmetry directions. With increase in pressure electron-phonon coupling varies differently in different directions and the overall effect may give rise to the softening of lattice. Measurement of phonon dispersions in different high symmetry directions by x-ray/neutron inelastic scattering measurements on single crystals of these systems would give a correct picture of evolution of phonons with pressure.

4. Conclusion

In this study we report a structural transformation from tetragonal to orthorhombic phase in Fe_2B at ~ 6.3 GPa for the first time. Further our study reveals a co-existing pressure regime of tetragonal and orthorhombic phases of Fe_2B up to 20 GPa. However, FeB was found to remain stable in orthorhombic phase up to the pressure of 24 GPa. Our analysis indicate that the dominant contribution to the temperature dependent resistivity in these systems arise from the electron-phonon scattering, while electron-electron and electron-magnon interactions seems to be very small in this system. The decrease in Debye temperature may indicate phonon softening with increase of pressure in this system.

Acknowledgments

The authors thank members of HPPS for valuable discussions. They also thank IGCAR management for their support.

References

- [1] S. Sen, I. Ozbek, U. Sen, C. Bindal, *Surf. Coat. Technol.* 135 (2001) 173–177.
- [2] A.L. Ivanovskii, *Prog. Mater. Sci.* 57 (2012) 184–228.
- [3] Q. Gu, G. Krauss, W. Steurer, *Adv. Mater.* 20 (2008) 3620–3626.
- [4] A.N. Kolmogorov, S. Curtarolo, *Phys. Rev. B* 74 (2006) 224507.
- [5] V.V. Brazhkin, *High Press. Res.* 27 (2007) 333–351.
- [6] R. Kiessling, *Acta Chem. Scand.* 4 (1950) 209–227.
- [7] A.G. Van Der Geest, A.N. Kolmogorov, *Calphad* 46 (2014) 184–204.
- [8] L. Lanier, G. Metauer, M. Moukassi, *Microchim. Acta* 114 (1994) 353–361.
- [9] D.S. Kumar, R.S. Keshavamurthy, P. Mohanakrishnan, S.C. Chetal, *Nucl. Eng. Des.* 265 (2013) 1159–1165.
- [10] J. Nagamatsu, N. Nakagawa, T. Muranaka, Y. Zenitani, J. Akimitsu, *Nature* 410 (2001) 63–64.
- [11] B. Cristina, Y. Tsutomu, *Supercond. Sci. Technol.* 14 (2001) R115.
- [12] A.N. Kolmogorov, S. Shah, E.R. Margine, A.F. Bialon, T. Hammerschmidt, R. Drautz, *Phys. Rev. Lett.* 105 (2010) 217003.
- [13] H. Gou, N. Dubrovinskaia, E. Bykova, A.A. Tsirlin, D. Kasinathan, W. Schnelle, A. Richter, M. Merlini, M. Hanfland, A.M. Abakumov, D. Batuk, G. Van Tendeloo, Y. Nakajima, A.N. Kolmogorov, L. Dubrovinsky, *Phys. Rev. Lett.* 111 (2013) 157002.
- [14] L.H. Li, W.L. Wang, L. Hu, B.B. Wei, *Intermetallics* 46 (2014) 211–221.
- [15] B. Xiao, J. Feng, C.T. Zhou, J.D. Xing, X.J. Xie, Y.H. Cheng, R. Zhou, *Phys. B Condens. Matter* 405 (2010) 1274–1278.
- [16] M. Zhang, H. Yan, *Solid State Commun.* 187 (2014) 53–58.
- [17] C.E. Rodríguez Torres, F.H. Sánchez, L.A. Mendoza Zélis, *Phys. Rev. B* 51 (1995) 12142–12148.
- [18] B. Chen, D. Penwell, J.H. Nguyen, M.B. Kruger, *Solid State Commun.* 129 (2004) 573–575.
- [19] D.J. Joyner, O. Johnson, D.M. Hercules, D.W. Bullett, J.H. Weaver, *Phys. Rev. B* 24 (1981) 3122–3137.
- [20] D.J. Joyner, O. Johnson, D.M. Hercules, *J. Phys. F Met. Phys.* 10 (1980) 169.
- [21] O. Johnson, D.J. Joyner, D.M. Hercules, *J. Phys. Chem.* 84 (1980) 542–547.
- [22] C.T. Zhou, J.D. Xing, B. Xiao, J. Feng, X.J. Xie, Y.H. Chen, *Comput. Mater. Sci.* 44 (2009) 1056–1064.
- [23] P. Mohn, D.G. Pettifor, *J. Phys. C Solid State Phys.* 21 (1988) 2829.
- [24] B. Shukla, N.R.S. Kumar, M. Sekar, N.V.C. Shekar, *J. Instrum. Soc. India.* 46 (2016) 75–77.
- [25] A.P. Hammersley, S.O. Svensson, M. Hanfland, A.N. Fitch, D. Hausermann, *High Press. Res.* 14 (1996) 235–248.
- [26] A. Mani, N. Ghosh, S. Paulraj, A. Bharathi, C.S. Sundar, *Europhys. Lett.* 87 (2009) 17004.
- [27] A. Mani, A. Bharath, V.S. Sastry, T.S. Radhakrishnan, Y. Hariharan, in: K.G. Narayankhedkar (Ed.), *International Cryogenic Engineering Conference*, Narosa Publishing House, Bombay, 2000, pp. 615–619.
- [28] A.T. Satya, A. Mani, A. Arulraj, N.V.C. Shekar, K. Vinod, C.S. Sundar, A. Bharathi, *Phys. Rev. B* 84 (2011) 180515.
- [29] G. Paolo, B. Stefano, B. Nicola, C. Matteo, C. Roberto, C. Carlo, C. Davide, L.C. Guido, C. Matteo, D. Ismaila, C. Andrea Dal, G. Stefano de, F. Stefano, F. Guido, G. Ralph, G. Uwe, G. Christos, K. Anton, L. Michele, M.-S. Layla, M. Nicola, M. Francesco, M. Riccardo, P. Stefano, P. Alfredo, P. Lorenzo, S. Carlo, S. Sandro, S. Gabriele, P.S. Ari, S. Alexander, U. Paolo, M.W. Renata, *J. Phys. Condens. Matter* 21 (2009) 395502.
- [30] P. Blaha, K. Schwarz, P. Sorantin, S.B. Trickey, *Comput. Phys. Commun.* 59 (1990) 399–415.
- [31] J.P. Perdew, K. Burke, M. Ernzerhof, *Phys. Rev. Lett.* 77 (1996) 3865–3868.
- [32] H.J. Monkhorst, J.D. Pack, *Phys. Rev. B* 13 (1976) 5188–5192.
- [33] P.E. Blöchl, O. Jepsen, O.K. Andersen, *Phys. Rev. B* 49 (1994) 16223–16233.
- [34] A.C. Larson, R.B. Von Dreele, *Los Alamos National Laboratory Report LAUR*, 2000, pp. 86–748.
- [35] B. Toby, *J. Appl. Crystallogr.* 34 (2001) 210–213.
- [36] N.V.C. Shekar, M. Sekar, P.C. Sahu, *Phys. B* 443 (2014) 95–98.
- [37] M. Sekar, N.V.C. Shekar, S. Appalakondaiah, G. Shwetha, G. Vaitheeswaran, V. Kanchana, *J. Alloy. Compd.* 654 (2016) 554–560.
- [38] P.J. Brown, J.L. Cox, *Philos. Mag.* 23 (1971) 705–725.
- [39] W.Y. Ching, Y.-N. Xu, B.N. Harmon, J. Ye, T.C. Leung, *Phys. Rev. B* 42 (1990) 4460–4470.
- [40] A. Gueddouh, B. Bentría, I.K. Lefkaier, *J. Magn. Magn. Mater.* 406 (2016) 192–199.
- [41] T.G. Kumary, J. Janaki, A. Mani, S.M. Jaya, V.S. Sastry, Y. Hariharan, T.S. Radhakrishnan, M.C. Valsakumar, *Phys. Rev. B* 66 (2002) 064510.
- [42] N.V. Volkenshtein, V.P. Dyakina, V.E. Startsev, *Phys. Status Solidi (b)* 57 (1973) 9–42.
- [43] A. Bid, A. Bora, A.K. Raychaudhuri, *Phys. Rev. B* 74 (2006) 035426.
- [44] M. Kaveh, N. Wiser, *Adv. Phys.* 33 (1984) 257–372.
- [45] G.T. Meaden, *Electrical Resistance of Metals*, Plenum Press 1965.
- [46] K.H.P. Kim, J.-H. Choi, C.U. Jung, P. Chowdhury, H.-S. Lee, M.-S. Park, H.-J. Kim, J.Y. Kim, Z. Du, E.-M. Choi, M.-S. Kim, W.N. Kang, S.-I. Lee, G.Y. Sung, J.Y. Lee, *Phys. Rev. B* 65 (2002) 100510.
- [47] D.E. Bugaris, C.D. Malliakas, D.Y. Chung, M.G. Kanatzidis, *Inorg. Chem.* 55 (2016) 1664–1673.
- [48] L.S. Mazov, *Phys. Rev. B* 70 (2004) 054501.
- [49] C. Salame, G. Khoury, M. Aillerie, M. Ibrir, S. Berri, S. Alleg, R. Bensalem, *Energy Procedia* 36 (2013) 612–617.
- [50] B.D. Hanson, M. Mahnig, L.E. Toth, *Z. Naturforsch. Part a-Astrophysik Phys. Phys. Chem. A* 26 (1971), 739–&.
- [51] D.B. Sirdeshmukh, K.G. Subhadra, *Phys. Status Solidi (b)* 150 (1988) K11–K14.
- [52] M. Kumari, N. Dass, *Phys. Status Solidi (b)* 133 (1986) 101–110.